ELSEVIER

Journal of Power Sources 76 (1998) 180–185

JOURNAL OF POWER SOURCES

Characterization of lithiated natural graphite before and after mild oxidation

C. Menachem [a], Y. Wang [b], J. Flowers [c], E. Peled [a], S.G. Greenbaum [b,*]

[a] *School of Chemistry, Tel Aviv University, Tel Aviv 69978, Israel*
[b] *Physics Department, Hunter College of CUNY, New York, NY 10021, USA*
[c] *Physical Sciences and Computer Science Department, Medgar Evers College of CUNY, Brooklyn, NY 11225, USA*

Received 10 July 1998; revised 4 October 1998; accepted 4 October 1998

Abstract

Partial oxidation of natural graphite utilized in lithium ion batteries was found to increase its reversible capacity, while decreasing the irreversible capacity. Several chemically distinct Li sites in lithiated graphite were identified by solid state ^{7}Li nuclear magnetic resonance (NMR): intercalated Li, and Li chemically bonded within the surface passivation layer or solid electrolyte interface (SEI). The partially oxidized graphite exhibited a third site, attributed to Li bonded to armchair, zigzag, or other edge sites in the carbon. In addition, the NMR signal from the SEI in the partially oxidized graphite is consistent with earlier work suggesting that oxidation lays the foundation for a chemically bonded SEI that is implicated in improved electrochemical performance. Electron paramagnetic resonance (EPR) signals observed in lithiated graphite are attributed to conduction electrons, as noted by other authors. EPR in unlithiated graphite, however, failed to detect a correlation between possible radical sites to which Li could bond and excess Li capacity in the partially oxidized graphite.

Keywords: Lithium ion battery; Graphite electrode; Enhanced capacity; Nuclear magnetic resonance (NMR)

1. Introduction

Lithiated carbons have been widely investigated during the last decade as a replacement for the lithium metal anode in lithium rechargeable batteries [1]. In order to decrease the energy density lost by this replacement, the capacity of lithium in carbons must be maximized. The theoretical reversible capacity of lithium in graphite is 372 mA h/g (or LiC_6). Recently, it was found that the reversible lithium capacity of some disordered carbons is much higher than this theoretical capacity and values as high as 1900 mA h/g have been reported [2–4]. However, compared to graphite, high deintercalation potential, high irreversible capacity and poor cycle life renders many of these disordered carbons impractical for use in commercial Li-Ion batteries.

It was also found that mild oxidation of graphite improves the performance of Li/Li_xC_6 cells: the irreversible capacity was decreased, the cycle life was improved and the reversible lithium capacity was increased up to 446 mA h/g (or $Li_{1.2}C_6$) [5–10].

To explain the extra lithium capacity in carbon and graphite, several suggestions have been proposed such as occupation of lithium in nearest neighbor sites [11], formation of lithium clusters inside nanoscopic cavities [12], adsorption of lithium on both sides of the basal plane [4] and accommodation of lithium in different internal and external edge sites by electrochemical reaction of lithium ion with different edge groups or edge free radicals [3,5,6,13,14].

The purpose of this work is to characterize the different sites of lithium in natural graphite (NG7) before and after mild oxidation with the use of solid state ^{7}Li nuclear magnetic resonance (NMR), and to examine a possible correlation between the extra lithium capacity and the presence of edge radicals, utilizing electron paramagnetic resonance (EPR) measurements. NMR has been employed productively in previous investigations to characterize the Li environment in graphite [15,16] and disordered carbons [11,17–20].

* Corresponding author. Tel.: +1-212-772-4973; Fax: +1-212-772-5390; E-mail: steve.greenbaum@hunter.cuny.edu

0378-7753/98/$19.00
PII: S0378-7753(98)00167-0

2. Experimental

Cell construction and disassembly as well as preparation of samples for NMR and EPR measurements were carried out inside a *VAC* argon glove box. The electrochemical measurements were carried out with the use of Li/Li_xC_6 cells. These cells consisted of a 12–15 cm^2 porous natural graphite (*NG7-Kansai Coke*) electrode and a lithium foil (*Foote Mineral*) supported (from both sides of the graphite electrodes) by a nickel Exmet screen, a *Celgard 2400* separator and electrolyte containing 1 M lithium hexafluoroarsenate ($LiAsF_6$) and 1:2 (v/v) mixture of ethylene carbonate (EC) and diethyl carbonate (DEC). The graphite electrodes were made by spreading paste which consists of 6.5% (w/w) Poly(vinylidene fluoride) (PVDF), 93.5% graphite powder and cyclopentanon on the nickel screen. Previous work in our laboratory has determined that PVDF does not react with lithium under normal charge or discharge conditions [21]. The electrodes were rolled to a thickness of 200 μm (about 50% porosity) and vacuum dried at 170°C for 3 h. The burnt graphite was prepared prior to electrodes preparation: NG7 powder was air-oxidized at 550°C for 30 min and lost 15% of its initial weight. The cells were cycled with the use of a 16-bit *Maccor 2000 Battery Tester* at 50 $\mu A/cm^2$ over a voltage range of 0.8–0.005 V. The cells were cycled one full intercalation–deintercalation cycle. At the second cycle, one set of cells was partially intercalated down to 120 mV and another set of cells was fully intercalated (down to 5 mV).

After 24 h at rest, the cells were disassembled. The graphite electrodes were washed in dimethyl carbonate (DMC) and vacuum dried at room temperature for 1 h. The lithiated graphite as well as the unlithiated graphite (the latter served as a reference for the EPR measurements) were separated from the nickel screen, crushed and inserted into *Aldrich* 5 mm (o.d.) × 22 mm Pyrex tubes for the NMR measurements and into *Wilmad* 5 mm (o.d.) × 10 mm quartz tubes for the EPR measurements. Both NMR and EPR tubes were sealed under argon (in a dry box) with polypropylene disks and *Torr Seal* cement. Both wide-line and magic angle spinning (MAS) NMR measurements were conducted on 500–700 mg samples with a *Chemagnetics CMX300* spectrometer operating at a ^7Li frequency of 116.9 MHz. A single-pulse sequence was employed for spectra acquisition, with a typical pulse width of 4 μs. The MAS rate was about 3 kHz, and the pyrex sample tubes were fitted with *Teflon* sleeves prior to insertion into the MAS rotor. Aqueous LiCl was employed as a chemical shift reference. X-band EPR measurements were performed with a Bruker EMX spectrometer on small samples (< 15 mg) to minimize microwave absorption difficulties associated with conductive materials. First-derivative spectra, employing a modulation amplitude of 0.10 G were obtained. The microwave power (20 mW), receiver gain, and modulation amplitude were kept constant for all of the samples in order to directly compare signal intensities. All NMR and EPR measurements were conducted at room temperature (21–24°C).

3. Results and discussion

The primary goal of this study is to identify the nature of the extra lithium in oxidized graphite. It was previously suggested that this extra lithium capacity is associated with electrochemical processes with EMF values in the 0.3–0.6 V range. For example, three possible reactions are listed below, along with their estimated E^0 values [7].

$$C\cdot + Li = C\text{–}Li\ (E_0 = 0.3\,V) \quad (1)$$

$$C\text{–}H + 2Li = C\text{–}Li + LiH\ (E_0 = 0.6\,V) \quad (2)$$

$$C\text{–}H + Li = C\text{–}Li + 1/2\,H_2\ (E_0 = 0.5\,V) \quad (3)$$

The latter two reactions, of course, assume the presence of bonded hydrogen, as found in a variety of incompletely graphitized carbons. From Figs. 1 and 2, it is apparent that for oxidized graphite, significant amounts of extra capacity are obtained at potentials higher than 0.12 V, during intercalation (Fig. 1), or higher than 0.15 V during deintercalation (Fig. 2). The reversible capacity of the pristine sample was the theoretical value for graphite: 372 mA h/g (or $x = 1$). The irreversible capacity was 120 mA h/g. The capacity of the pristine sample after intercalation to 120 mV was 78 mA h/g (or $x = 0.21$; Fig. 1). After mild oxidation (15% burn-off) the reversible capacity increased to 402 mA h/g (or $x = 1.08$; Fig. 2) and the irreversible capacity decreased to 90 mA h/g. The capacity of the partially oxidized (hereafter denoted as 'burnt') sample after intercalation to 120 mV was 89 mA h/g (or $x = 0.24$). Thus, there is a gain in capacity of about 12 mA h/g in

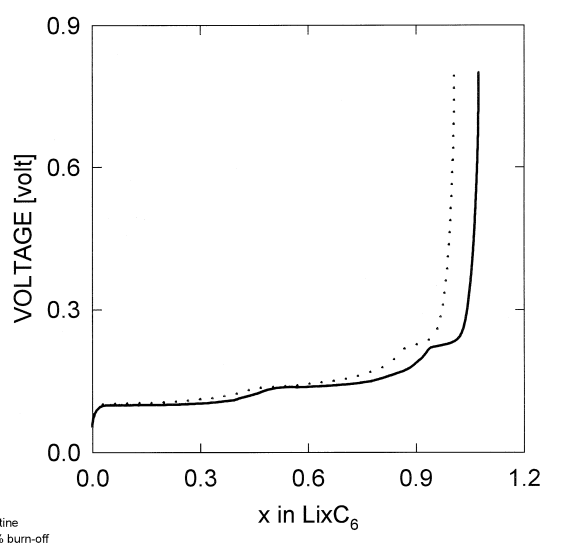

Fig. 1. Second intercalation curves (down to 120 mV cell potential) for pristine graphite (NG7) (dotted line) and 15% burn-off (burnt) NG7 (solid line).

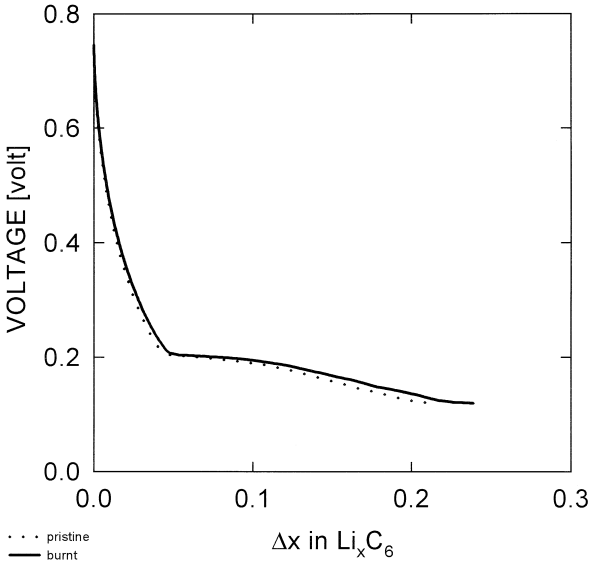

Fig. 2. First deintercalation curves for pristine NG7 (dotted line) and burnt NG7 (solid line).

this potential range, and more lithium can be inserted into these sites at lower potentials.

In order to identify the environment of the extra capacity lithium in burnt graphite, wide-line ^{7}Li NMR measurements of pristine graphite, lithiated to $x = 0.21$ (Li_xC_6), and burnt graphite, lithiated to $x = 0.24$, were carried out. The two spectra, displayed in Fig. 3, are similar in appearance, both being dominated by a strong central transition flanked by outer satellite transitions associated with a first-order electric quadruple interaction between the ^{7}Li nucleus and the axial electric field gradient surrounding the Li ion. Similar spectra for Li-intercalated graphite have been reported previously [15]. Both main peaks are centered at about 40 ppm, close to the 45 ppm Knight shift value reported for LiC_6 [15]. In addition to the intercalated Li signal, there is some NMR intensity centered around 0 ppm in both samples, considerably more so for the burnt graphite. Electrochemical lithiation of graphite (or other carbons) produces a surface layer, commonly referred to as the solid electrolyte interface (SEI), which arises from decomposition of electrolyte solvent [7]. This Li-containing surface layer constitutes the irreversible fraction of the total Li content. The SEI in graphite contains, in addition to polymerized solvent decomposition products [5,6,21], Li carbonate and semicarbonates [21,22], and therefore gives rise to an NMR signal at around 0 ppm [20]. The considerably larger feature, centered around 12–18 ppm, in the burnt graphite is attributed to the extra reversible lithium capacity in this material.

In order to gain additional information on the nature of this excess Li, high-resolution ^{7}Li MAS measurements were undertaken, and MAS spectra of both samples described above (pristine graphite lithiated to $x = 0.21$ and burnt graphite lithiated to $x = 0.24$) are shown in Fig. 4. The high-resolution spectra reveal additional intensity in the burnt graphite compared to pristine graphite, at least some of which is associated with the excess Li capacity in the former, more clearly than the wide-line spectra do. The excess Li spectral component appears as a broad line centered at around 14 ppm. In addition, there is greater intensity in the 0 ppm region in the burnt graphite compared to the pristine graphite. Both wide-line and MAS ^{7}Li NMR measurements on fully intercalated graphite, corresponding to LiC_6 for pristine graphite and $Li_{1.08}C_6$ for burnt graphite, were also performed (spectra not shown). The spectra are qualitatively similar to those for the partially lithiated samples (Figs. 3 and 4), except that the SEI and excess Li (the latter in only the burnt sample) contribution to the signal is considerably smaller than that of the intercalated Li, due to the higher degree of lithiation in these samples. The 14 ppm feature is almost unobservable in the fully lithiated burnt graphite, which implies that the extra Li capacity is associated with potentials larger than 0.1 V, and not with potentials close to 0, vs. Li.

The mechanism by which partial oxidation increases the reversible Li capacity is believed to be related to Li bonding at edge atomic sites, such as zigzag and armchair

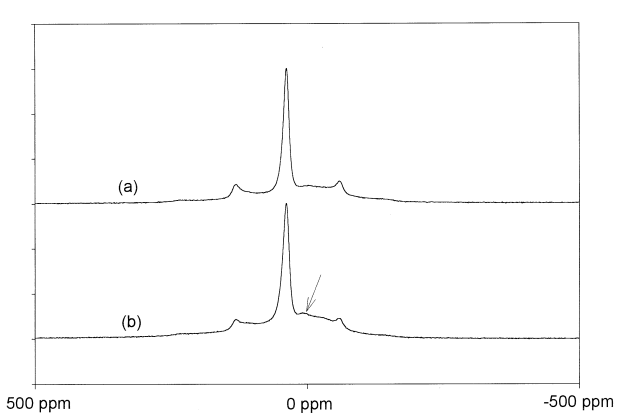

Fig. 3. Wide-line ^{7}Li NMR spectra of lithiated pristine NG7, $Li_{0.21}C_6$ (a) and lithiated burnt NG7, $Li_{0.24}C_6$ (b). Arrow indicates spectral component associated with excess lithium capacity.

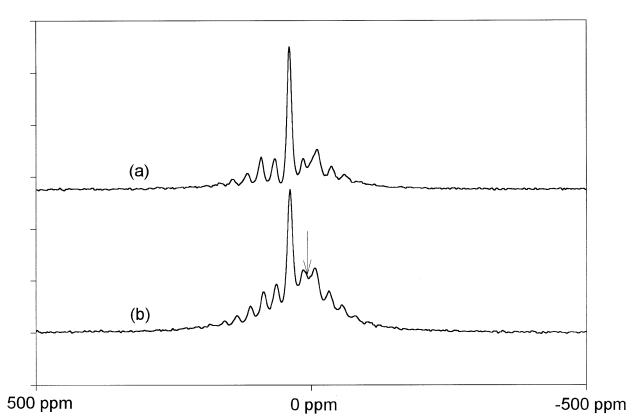

Fig. 4. High-resolution MAS ^{7}Li NMR spectra of lithiated pristine NG7, $Li_{0.21}C_6$ (a) and lithiated burnt NG7, $Li_{0.24}C_6$ (b). Arrow indicates spectral component associated with excess lithium capacity.

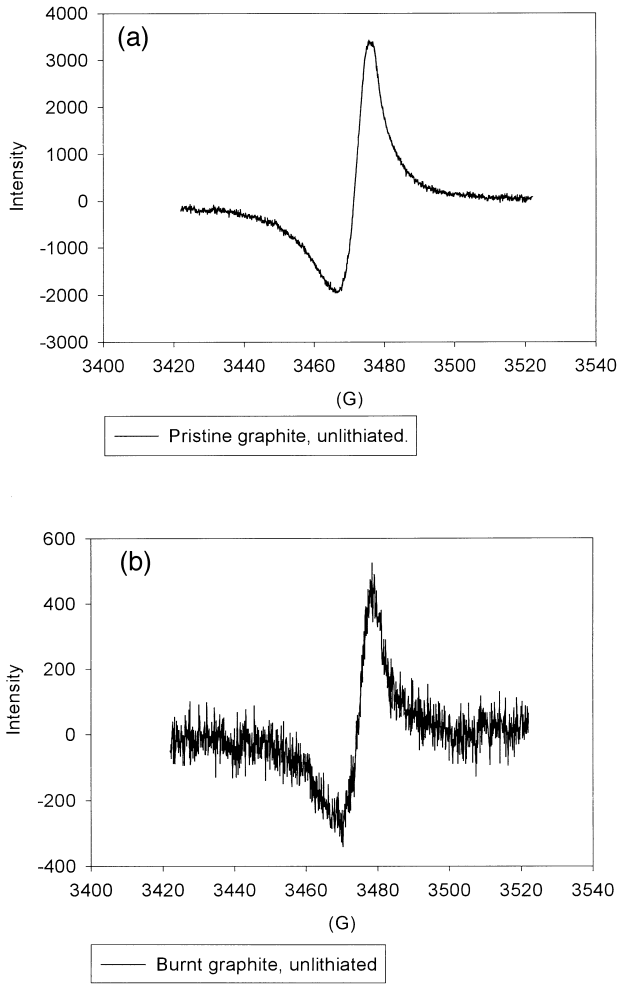

Fig. 5. First-derivative EPR signal for unlithiated NG7: (a) pristine; (b) burnt.

sites, as opposed to intercalation between graphene sheets. In particular, oxidation proceeds most rapidly at the zigzag and armchair sites, and results in the formation of COOH acid groups, which have been detected directly (along with CH, COH and C=O groups) by X-ray photoelectron spectroscopy [9]. These acid groups, in turn, are transformed into a chemically bonded SEI during the first Li insertion step [5–7]. The larger NMR intensity around 0 ppm in the burnt sample (Fig. 4) is attributed to either a thicker SEI, or an SEI that is richer in Li salts (at the expense of organic decomposition products), compared to the pristine graphite case. This conclusion is supported by previous X-ray photoelectron spectroscopy results, which found evidence of both thicker SEI and higher Li salt content in burnt graphite compared to pristine graphite [22]. The fact that the irreversible capacity of the former is smaller than that of the latter [7–9] can be taken as evidence that the SEI formation process is more efficient in burnt graphite.

Previous work on Li insertion in disordered hard carbon suggested that excess Li capacity was associated with covalently bonded Li [20]. A possible mechanism for Li reaction resulting in a covalent C–Li bond involves the presence of carbon radical sites or dangling bonds [as described in reaction (1)]. In order to test this hypothesis, EPR spectra of pristine and burnt graphite, both unlithiated and lithiated are presented in Figs. 5 and 6. For the unlithiated case (Fig. 5), EPR intensity is significantly reduced upon oxidation. Although the spin density is directly related to the integrated spectral absorption (or the twice-integrated EPR derivative signal), the derivative EPR spectrum itself is sufficient to monitor changes in spin density in cases where the line shape doesn't change appreciably. Taking into account the different line widths, and sample quantities, the burnt sample has a lower spin density by about a factor of 5–8. The major source of error here arises from inaccurate determination of relative sample quantities. The experimental g-factors for the unlithiated graphite samples, are: $g = 2.0056$ for pristine and $g = 2.0052$ for burnt graphite, and 2.0017 for lithiated pristine and 2.0015 for lithiated burnt graphite. The line widths, calculated from the separation of the derivative peaks are 7.7 G and 6.8 G for the pristine and burnt unlithiated samples, respectively. As demonstrated in Fig.

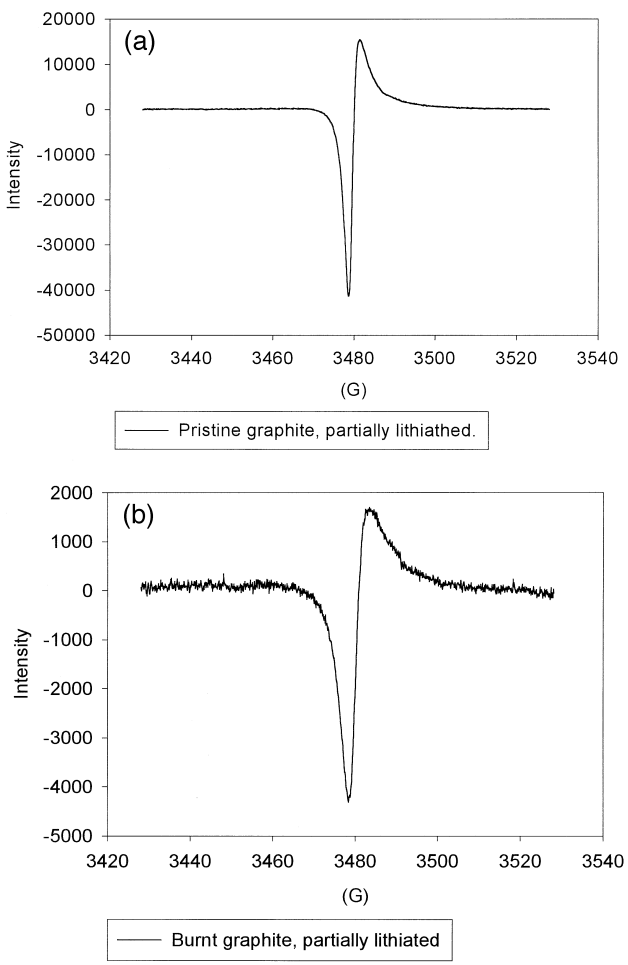

Fig. 6. First derivative EPR signal for lithiated NG7: (a) pristine, $Li_{0.21}C_6$; (b) burnt, $Li_{0.24}C_6$.

6, the EPR signal of lithiated graphite is considerably narrower than that of unlithiated graphite, 2.8 G for pristine and 3.9 G for burnt lithiated graphite, respectively. In addition, the overall integrated intensity (again taking into account the difference in line widths and sample amounts —larger quantities of the lithiated samples were employed) of lithiated pristine graphite is over a factor of two larger than that of the burnt lithiated graphite. The lithiated graphite results (g-values and line widths) are consistent with previously reported EPR results for graphite intercalation donor compounds, in which the resonance signal is attributed to conduction electrons [23]. The reason for the observed difference in relative spin densities of the lithiated samples is then unclear at this time (they should have comparable conduction electron densities), but may be related to microwave skin depth phenomena associated with metallic samples. Although the powder grain sizes of both samples were comparable, it is possible that even small differences could lead to different microwave absorption characteristics for highly conductive materials.

Although it can be concluded on the basis of the NMR results that mild oxidation of graphite produces changes in surface-bonded structures that improve the reversible Li capacity, the EPR results do not support a mechanism by which the excess Li bonds to radical sites [reaction (1)]. If, in fact, the EPR signal in the unlithiated graphite is due to carbon radicals which might then act as Li bonding sites, then mild oxidation reduces rather than increases their concentration in graphite prior to lithiation, as per the factor of 5–8 difference in signal intensities between the pristine and burnt graphite. More likely, the observed EPR signal in unlithiated graphite also contains contributions from conduction electrons, as deduced from much earlier studies [24]. Therefore, although the carbon radical/lithium uptake mechanism cannot be ruled out completely at this time, the current EPR results do not provide evidence for it. One possible avenue towards a more definitive EPR result is to perform variable temperature measurements, which might better separate conduction vs. non-conduction resonance signals.

4. Conclusions

Mild oxidation of natural graphite was undertaken in order to improve its properties as an anode material in lithium ion batteries. Samples oxidized to 15% mass loss exhibited an 8% increase in reversible lithium capacity, and about a 25% decrease in irreversible lithium capacity, relative to pristine graphite. Solid state ^{7}Li NMR measurements identified two kinds of Li sites in lithiated pristine graphite: Li intercalated between graphene planes, with $\sim$ 40 ppm Knight shift (relative to aqueous LiCl), and Li chemically associated with the solid electrolyte interface (SEI), characterized by a chemical shift around 0 ppm. The burnt graphite also exhibited a feature around 14 ppm, correlated with the excess Li and attributed to Li bonded to armchair, zigzag, or other edge sites. In addition, the ^{7}Li signal associated with the SEI was more intense in the burnt graphite, consistent with earlier indications that mild oxidation prior to lithiation results in a thicker and more salt-rich SEI.

EPR measurements were performed in order to test the hypothesis that excess Li could bond to radical sites. However, the oxidized graphite yielded an even smaller spin density than the pristine graphite. Thus, the EPR measurements do not support this conjecture at the present time.

Acknowledgements

This work was supported by grants from the Israeli Ministry of Science, the US Department of Energy, and the US Office of Naval Research. Funds to purchase the EPR spectrometer utilized in this investigation were provided by a US Army Research Office grant, under the *Defense University Research Instrumentation Program.*

References

[1] J.R. Dahn, A.K. Sleigh, H. Shi, B.M. Way, J. Weydanz, J.N. Reimers, Q. Zhong, U. von Sacken, in: G. Pistoia (Ed.), Lithium Batteries—New Materials, Developments and Perspective, Elsevier (1994) p. 1.
[2] Y. Liu, J.S. Xue, T. Zheng, J.R. Dahn, Carbon 34 (1996) 194.
[3] J.R. Dahn, T. Zheng, Y. Liu, J.S. Xue, Science 297 (1995) 590.
[4] R. Yazami, M. Descamps, 13th International seminar on primary and secondary battery technology and application, Florida International Seminar, Boca Raton, FL, March 4–7 (1996).
[5] E. Peled, Rechargeable lithium and lithium-ion batteries, in: S. Megahed, B.M. Barent, Xie (Eds.), The Electrochem. Soc. Proceedings Series 94-28 (1995) 1.
[6] E. Peled, D. Golodnitsky, G. Ardel, C. Menachem, D. Bar-Tow, V. Eshkenazi, Proceedings of the 1995 MRS Spring Meeting 393 (1995) 209.
[7] E. Peled, C. Menachem, D. Bar-Tow, A. Melman, J. Electrochem. Soc. 143 (1996) L4.
[8] C. Menachem, E. Peled, L. Burstein, 37th Power Sources Conference, NJ, June (1996) 208.
[9] C. Menachem, E. Peled, L. Burstein, Y. Rosenberg, J. Power Sources 68 (1997) 277.
[10] Y. Ein-Eli, V.R. Koch, J. Electrochem. Soc. 144–9 (1997) 2968.
[11] K. Sato, M. Noguchi, A. Demachi, N. Oki, M. Endo, Science 264 (1994) 556.
[12] A. Mabuchi, K. Tokumitsu, H. Fujimoto, T. Kasah, J. Electrochem. Soc. 142 (1995) 1041.
[13] T. Zheng, Y. Liu, E.W. Fuller, S. Tseng, U. von Sacken, J.R. Dahn, J. Electrochem. Soc. 142 (1995) 2581.
[14] P. Papanek, M. Radosavljvic, J. Fischer, Chem. Mater. 8 (1996) 1519.
[15] J. Conard, H. Estrade, Mater. Sci. Eng. 31 (1977) 173.
[16] J. Conard, V. Nalimova, D. Gerard, Mol. Cryst. Liq. Cryst. 245 (1994) 25.

[17] Y. Mori, T. Iriyama, T. Hashimoto, S. Yamazaki, F. Kawamaki, H. Shiroki, T. Yamabe, J. Power Sources 56 (1995) 205.
[18] K. Tatsumi, T. Akai, T. Imamura, K. Zaghib, N. Iwashita, S. Higuchi, Y. Sawada, J. Electrochem. Soc. 143 (1996) 1923.
[19] N. Takami, A. Satoh, T. Ohsaki, M. Kanda, Electrochim. Acta 42 (1997) 2537.
[20] Y. Dai, Y. Wang, V. Eshkenazi, E. Peled, S.G. Greenbaum, J. Electrochem. Soc. 145 (1998) 1179.
[21] D. Bar-Tow, E. Peled, L. Burstein, J. Electrochem. Soc., submitted.
[22] O. Chusid, Y. Ein-Ely, D. Aurbach, J. Power Sources 43 (1993) 47.
[23] M.S. Dresselhaus, G. Dresselhaus, Adv. Phys. 30 (1981) 139.
[24] L.S. Singer, G. Wagoner, J. Chem. Phys. 37 (1962) 1812.